Int. J. Heat Mass Transfer. Vol. 13, pp. 901–909. Pergamon Press 1970. Printed in Great Britain

VARIABLE VISCOSITY ENTRANCE-REGION FLOW OF NON-NEWTONIAN LIQUIDS

A. A. MCKILLOP, J. C. HARPER, H. J. BADER and A. Y. KORAYEM
University of California, Davis, California, U.S.A.

(*Received* 29 *August* 1968 *and in revised form* 3 *November* 1969)

Abstract—A numerical solution was obtained for the problem of flow of a non-Newtonian fluid with temperature-dependent viscosity in the entrance region of a round tube. The solution, which is based on an integral boundary layer approach in the immediate entrance region and a finite difference scheme farther downstream, gives pressure drops and Nusselt numbers as functions of downstream distance for a uniform entering velocity and a constant tube wall temperature. A power-law model with an Arrhenius-type temperature dependency was used to represent the fluid. Results are presented in the form of correlations in terms of the parameters n, Pr and H (the ratio of the wall viscosity to entering viscosity) from which numerical values can be obtained if values of the viscosity constants of the fluid are known.

NOMENCLATURE

a, coefficient in velocity profile;
c, heat capacity;
D, diameter;
g_i, coefficients of correlation equation (10);
H, $\exp(T'/T_w - T'/T_e)$;
K, non-Newtonian coefficient of consistency in power-law expression;
k, thermal conductivity;
n, non-Newtonian fluid behavior index in power-law expression;
Nu, Nusselt number, hD/k;
p, pressure;
p^*, dimensionless pressure, $p/\frac{1}{2}\rho u_m^2$;
Pr, modified Prandtl number, $(Kc/k)(r_0/u_m)^{1-n}$;
Re, Reynolds number $(\rho u_m^{2-n} r_0^n)/K$;
r, radial distance;
r_0, tube radius;
r^*, dimensionless radial distance, r/r_0;
T', exponential viscosity-temperature coefficient;
T, absolute temperature;
u, axial velocity;
u^*, dimensionless axial velocity, u/u_c;
u_1, dimensionless axial velocity, u/u_m;
u_c, core velocity;
u_m, average velocity;
v, radial velocity;
v_1, dimensionless radial velocity, $Re\, v/u_m$;
x, axial distance;
x^*, dimensionless axial distance, $x/r_0 Re$;
x_0, dimensionless axial distance, x^*/Pr;
y_p, variable defined by equation (10);
z, variable defined by equation (10).

Greek letters

δ, momentum boundary-layer thickness;
δ_t, thermal boundary-layer thickness;
δ^*, dimensionless thickness, δ/r_0;
δ_t^*, dimensionless thickness, δ_t/r_0;
η, dimensionless distance, $(r_0 - r)/\delta$;
η_t, dimensionless distance, $(r_0 - r)/\delta_t$;
θ, dimensionless temperature, $(T - T_e)/(T_w - T_e)$;
ρ, density;
τ, shear stress;
τ^*, dimensionless shear stress, $Re\, \tau/\rho u_m^2$.

Subscripts

e, entrance;
f, fully developed;
w, wall.

IN RECENT years interest has increased in the flow and heat-transfer characteristics of non-Newtonian fluids because of their importance in chemical and food-processing industries. This paper stems from a general study of liquid food products with gross properties attributed to pseudoplastic non-Newtonian fluids. Primary concern is with the laminar regime, since the high viscosity (or consistency) of such liquids rules out turbulent flow in most processing applications. At the same time, Prandtl numbers are high, and there is likely to be a strong dependency of viscosity on temperature. From the physical standpoint, the high Prandtl number means that thermal development will be slow. Fully developed flow may not be achieved in many commercial applications, and entrance-region effects can be important. Of primary interest to the engineer is the gross effect of such flow (i.e. pressure drop and heat-transfer coefficients) rather than details of velocity and temperature profiles. The following discussion is therefore concerned with the influence of variable viscosity on the overall pressure drop and local heat-transfer coefficient for non-Newtonian liquids in laminar flow in round tube with a uniform entering velocity profile.

The solutions presented are for constant wall temperature; however, the effect of variable viscosity should be at least qualitatively independent of the heat-supply mechanism. McKillop [1] showed that, for constant-property solutions in the entrance region, the ratio of constant-heat-flux to constant-wall-temperature Nusselt numbers was approximately 1·25 over a wide range of variables for both Newtonian and non-Newtonian liquids. The analysis is based on rheological behavior that is described by the power-law equation

$$\tau = K\, e^{T'/T} \left(-\frac{\partial u}{\partial r}\right)^n. \qquad (1)$$

Equation (1) couples the momentum and thermal energy equations so that they must be solved simultaneously. Harper and El Sahrigi [2] present information from several sources showing that equation (1) adequately represents the behavior of a variety of food products.

Previous solutions to flow inside circular tubes have been either by the integral boundary-layer technique or a direct finite difference solution of the governing equations themselves. As long as the boundary-layer thickness is small compared to the tube radius, the integral method gives values of the pressure drop which are in excellent agreement with experimental data (e.g. Campbell and Slattery [3], Bogue [4], and Shapiro *et al.* [5]). The finite-difference technique is valid once the boundary layer has reached sufficient thickness to include a large number of grid points. Thus, it is valid a sufficient distance downstream, but gives results for pressure drop and local heat-transfer coefficients which are substantially in error in the immediate vicinity of the entrance. The results presented here are based on a combination of both methods. Frequently, there was a region of overlap at intermediate distances where the two methods were in agreement.

Rosenberg and Hellums [6] used the finite difference scheme to solve the problem of temperature-dependent viscosity flow of Newtonian fluids in the entrance region. They included no pressure drop information and their results for high Prandtl numbers were unfortunately obtained only for regions where the numerical method appears to give erroneous results. Test [7] used the same numerical technique for Newtonian liquids with a parabolic entering velocity profile. His results for both pressure drop and Nusselt number, which were essentially asymptotic values, could be presented in the form of Sieder–Tate type corrections. The analytical model was substantiated by good agreement between experimental and calculated velocity profiles. A similar solution to Test's for non-Newtonian liquids was obtained by Christiansen and Craig [8] but

under more severe restrictions. A constant-property solution for non-Newtonian fluids in the entrance region was obtained by McKillop [1].

In addition to the above analyses, several existing solutions form limits within which the current analysis must fall. Sufficiently far from the entrance, the effects of both variable viscosity and developing flow will die out, so that the slope of the pressure-drop curve and the asymptotic Nusselt numbers should correspond to values obtained in constant-property solutions. In the immediate vicinity of the entrance, on the other hand, the solution should be approximated by the flat-plate solution. Seban [9], who solved this problem for temperature-dependent viscosity flow of Newtonian liquids, concluded that prediction of local heat-transfer coefficients can be made from constant-property results if the Prandtl number is based on the wall viscosity. Experimental data to confirm the results of the present analysis are non-existent.

The continuity, momentum and thermal energy equations from which the velocity and temperature profiles are ultimately defined are the same for both the boundary layer and finite difference methods and can be written in dimensionless form as

$$v_1 = -\frac{1}{r^*}\int_0^{r^*} r^* \frac{\partial u_1}{\partial x^*}\,dr^* \tag{2}$$

$$u_1\frac{\partial u_1}{\partial x^*} + v_1\frac{\partial u_1}{\partial r^*} + \frac{1}{2}\frac{dp^*}{dx^*} = \frac{1}{r^*}\frac{\partial}{\partial r^*}(r^*\tau^*) \tag{3}$$

$$u_1\frac{\partial \theta}{\partial x^*} + v_1\frac{\partial \theta}{\partial r^*} = \frac{1}{r^* Pr}\frac{\partial}{\partial r^*}\left(r^*\frac{\partial \theta}{\partial r^*}\right). \tag{4}$$

In the above equations, and throughout the entire paper, the Prandtl and Reynolds numbers are based on the wall temperature and are given by the expressions

$$Pr = \frac{cK}{k}\left(\frac{r_0}{u_m}\right)^{1-n} \qquad Re = (\rho u_m^{2-n} r_0^n)/K.$$

For the boundary-layer solution, equations (3) and (4) are integrated over the radius. The necessary boundary condition defining the core velocity is obtained by writing the mechanical energy equation to account for all viscous dissipation in the boundary layer, as follows:

$$\frac{d}{dx^*}\int_0^1 u_1^3 r^*\,dr^* + \frac{d}{dx^* p^*}\int_0^1 u_1 r^*\,dr^* - 2\int_0^1 r^*\tau^*\left(\frac{\partial u_1}{\partial r^*}\right)dr^* = 0. \tag{5}$$

A fourth degree polynomial is chosen to represent the velocity profile in order to allow for the inflection that can occur with cooling, whereas a third degree polynomial was sufficient for the temperature profile. The resulting equations, obtained in the usual manner, are

$$\frac{u}{u_c} = a(x^*)\eta + 3(2-a)\eta^2 + (3a-8)\eta^3 + (3-a)\eta^4, \tag{6}$$

where the coefficient, a, is a function of x^*, and

$$\theta = 1 - \frac{6\eta_t}{4+\delta_t^*} - \frac{3\delta_t^*}{4+\delta_t^*}\eta_t^2 + \frac{2(1+\delta_t^*)}{4+\delta_t^*}\eta_t^3. \tag{7}$$

Details of the solution of the boundary-layer equations are given by Bader [10].

For the finite-difference solution, equations (2)–(4) were solved by an implicit method. In order to preserve linearity, the coefficients of the derivatives were evaluated at the upstream position. The ensuing matrix form of the equations was solved with an algorithm similar to that used for a tri-diagonal set. Local Nusselt numbers were calculated from the wall temperature gradient and the difference between the wall and mean fluid temperatures, and the pressure drop was obtained from the following macroscopic momentum balance equation

$$\Delta p^*/2 = 2\int_0^1 u_1^2\,dr^* - 1 - \int_0^{x^*}\tau_w^*\,dx^*. \tag{8}$$

Bader [11] presents details of the finite-difference solution.

RESULTS AND DISCUSSION

The independent variables for both the boundary layer and finite-difference solutions are Pr; the power law exponent n; and two temperature parameters, one involving the difference between the wall and entering temperatures, and the other accounting for the effect of the consistency-temperature exponent T'. In numerical solutions over a wide range of variables, it was found that the effects of the latter two parameters can be combined into a single parameter H with an error no greater than 5 per cent. The parameter H represents the ratio of the temperature-dependent factor of the apparent viscosity at the wall to that at the entrance and, by equation (1), is given by the expression

$$H = [\exp(T'/T_w)]/[\exp(T'/T_e)] = \exp(T'/T_w - T'/T_e). \quad (9)$$

H is thus greater than 1·0 for cooling, and less than 1·0 for heating. Data for typical food materials [2] show that a temperature difference of 200°F would correspond to a value of H of about 3·0 (or 0·33).

As the analysis progressed, it became apparent that there are advantages in comparing results on the basis of Prandtl numbers calculated at the wall temperature rather than the entering temperature of the fluid. The numerical solutions, however, had originally been set up on the basis of the entering Prandtl number, and results were obtained corresponding to entering Prandtl numbers of 1·0, 10, 100 and 1000 at H of 5·0, 3·2, 1·6, 1·0, 0·664, 0·333 and 0·2. Because of limitations of the program, solutions for the boundary-layer method were more difficult to obtain as n decreased, as Pr increased, and as H departed from unity. Specifically, the number of heating runs was quite limited, and no valid results were obtained for $n = \frac{1}{3}$. Even though results were missing in some regions, it was possible to extrapolate or interpolate curves with a reasonable degree of confidence to be consistent with the available data.

Pressure drop

With the conventions used here, the pressure drop in fully developed constant-property flow is given by the expression

$$\Delta p^* = 4\left(\frac{1+3n}{n}\right)^n x^*.$$

For $n = 1$, this expression reduces to $\Delta p^* = 16x^*$. If Δp^* is plotted against the right-hand side of the above expression divided by 16, instead of against x^*, the fully developed constant-temperature flow lines for all values of n will coincide with the case of Newtonian flow, and the curves for all combinations of n, Pr and H will approach a common asymptote. Figure 1 is such a plot of constant-property ($H = 1$) pressure drops for various values of n.

The solution is in good agreement with the experimental data of Korayem [12] for n of 1·0 and 0·45, as shown by the points on the figure. Shapiro *et al.* [5] present both analytical and experimental results for $n = 1$. Above x^* of

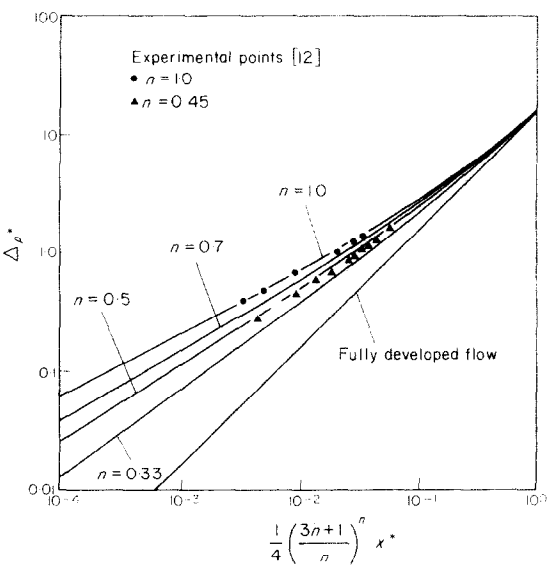

FIG. 1 Constant property pressure drop.

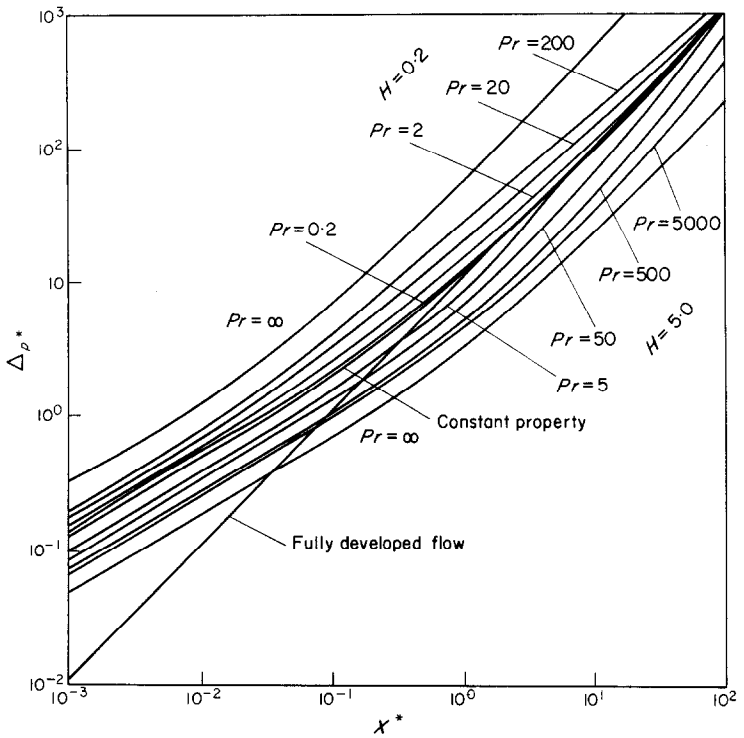

FIG. 2. Variable property pressure drop for $n = 0{\cdot}7$.

4×10^{-3}, which represents the upper limit of their experimental data, their analytical results and the present solution are in essentially complete agreement. At lower values of x^*, the slope of the line for $n = 1$ on Fig. 1 is 0·52, whereas both the experimental and analytical results of Shapiro *et al.* agree with the usual theoretical slope of 0·50. Accordingly, there is a small discrepancy between the magnitudes of the pressure drops at lower values of x^*.

Figure 2 is a plot of pressure drop results showing the effects of both heating and cooling for $n = 0{\cdot}7$ and with H of 5 and 0·2. These results are typical of all those obtained, and the following general observations can be made:

1. Cooling results in a lower pressure drop and heating in a higher pressure drop than constant temperature flow. Accordingly, the cooling lines approach the asymptotic constant property line from below and heating lines from above.

2. At smaller values of x^*, all lines become straight and parallel to the constant property line. Since the constant property line is independent of Pr, all lines for a particular n are parallel in this region, regardless of the value of Pr or H.

3. The effect of heating or cooling increases as Pr increases.

To compare the effects of cooling with constant-property behavior, we consider the case in which the fluid enters at a higher temperature and is cooled toward the constant value. For cooling, the average viscosity in the developing momentum boundary layer at any downstream point will always be lower than for a constant-property fluid having a viscosity corresponding to the wall temperature. Because of the lower viscosity in the boundary layer, where the viscous dissipation is occurring, the pressure drop over any given distance from the entrance will be less for cooling. The converse of this situation applies to heating.

As Pr increases, the thermal penetration is smaller, and the effect described above of either heating or cooling is accentuated. In the limit of infinite Pr, there is no thermal penetration, and the flow would be that of constant property corresponding to the entering temperature. Since x^* is directly proportional to the viscosity (or consistency coefficient) of the fluid, using the entering temperature instead of the wall temperature in Fig. 2 merely has the effect of shifting the lines horizontally by a factor of H. Accordingly, the infinite Pr lines on Fig. 2 were obtained by applying a factor of 5 to the constant property line for cooling and 0·2 for heating. At the opposite limit of zero Pr, the fluid is heated to the wall temperature instantaneously, and the pressure drop corresponds to the constant property line.

To provide a convenient form of presentation, the data were correlated in terms of equation (10) by a least squares method,

$$y_p = \sum_{1}^{s} g_i z^i \qquad (10)$$

where $y_p = \ln(\Delta p^*/\Delta p^*_{x^*=1})$ and $z = \ln x^*$. The coefficients of this equation are presented in a separate tabulation.† All data are correlated over the region $10^{-3} < x^* < 40$ for heating and $10^{-2} < x^* < 40$ for cooling. Below the minimum value, the lines parallel the constant-property solution. The constant-property solution is a straight line for $x^* < 10^{-3}$. Thus if pressure drops for values of x^* less than minimum are needed, one can project backwards, from the minimum point, at a slope equal to that of the constant-property line. The correlation equation represents the data with a maximum deviation less than 3 per cent.

† Tabular material is deposited as document NAPS-00620 with the ASIS-National Auxiliary Publications Service, c/o CCM Information Sciences, Inc., 22 West 34th Street, New York, N.Y. 10001 and may be obtained for $1.00 for microfiche or $3.00 for photocopy.

Heat transfer

Although Nusselt numbers are most conveniently represented on a dimensionless basis in terms of $x_0(=x^*/Pr)$, the parameter x^* is a more direct measure of the physical tube length. There is little practical interest in values of x^* below about 10^{-3}, which corresponds to a tube length equal to the radius at the upper limit of laminar flow. Where boundary layer solutions were available, there was no difficulty in extending the plots well below this value of x^*. The finite difference solution was generally valid down to x_0 ranging from about 10^{-4} to 10^{-2}, corresponding to much higher values of x^* at the higher Prandtl numbers. Where boundary layer solutions could not be completed, as in the case of many of the heating runs, there was some uncertainty in extrapolating Nusselt number plots to the desired lower limit of x^*. There was judged to be insufficient basis for presenting any heat transfer results for $n = \frac{1}{3}$, since no boundary layer data were obtainable. Probably because of grid size limitations, the finite difference solution appeared to give high Nusselt numbers for both constant property and heating for all values of n at $Pr = 1{\cdot}0$. The results tabulated† for this condition were obtained by making adjustments to give curves that appeared to be consistent with the other data.

At a sufficient distance downstream, Nusselt numbers for both heating and cooling must approach the asymptotic value that corresponds to constant-property flow with a fully developed entering velocity profile. These asymptotic values are listed in Table 1. If the entrance region data for constant-property fully developed entering velocity profiles are plotted as the ratio of Nu to the asymptotic value, the results for all values of n fall on a single line. This line, corresponding to the standard Graetz solution, constitutes the limiting case of infinite Prandtl number for constant-property flow. Below x_0 of 5×10^{-3} it can be represented by the equation

$$Nu_f/Nu_\infty = 0{\cdot}413\, x_0^{-0{\cdot}344}. \qquad (11)$$

† Refer to previous footnote.

Table 1.
Asymptotic local Nusselt numbers

n	Nu
1·0	3·66
0·7	3·79
0·5	3·94
0·4	4·07
0·33	4·18

At higher values of x_0, any of the lines for Pr of 100 or 1000 given by the tabulated coefficients can be used for the fully developed line.

The fact that the constant-property fully developed flow lines are the same for all values of n (when referred to the asymptotic limit) suggests the possibility of a simplification by using these lines as reference in plotting the constant-property Nusselt number results. It was found that if Nu/Nu_f is plotted against x^* rather than x_0, the lines for each n at Pr of 10, 100 and 1000 coincide with a maximum deviation of 3 per cent. All of these lines come together in the portion of the fully-developed line corresponding to equation (11). The lines for Pr of 1·0 merge with the fully developed line at a higher value of x_0, where it is no longer straight on a logarithmic plot, and thus do not coincide with the higher Pr results. The numerical results of the plot for the higher Pr are given in Table 2. These values, together with the fully developed flow line, permit the constant-property Nu to be obtained for any Pr.

Table 2. *Ratio of constant-property to fully-developed Nusselt numbers*

n	1·0	0·7	0·5
x^*			
10^{-4}	1·78	2·23	2·59
2	1·64	1·99	2·27
3	1·58	1·84	2·11
4	1·52	1·78	2·00
6	1·46	1·66	1·85
8	1·41	1·59	1·76
10^{-3}	1·36	1·53	1·68
2	1·27	1·37	1·48
3	1·21	1·30	1·38
4	1·18	1·25	1·32
6	1·14	1·19	1·25
8	1·11	1·15	1·20
10^{-2}	1·09	1·13	1·17
2	1·04	1·06	1·08
3	1·02	1·03	1·04
4	1·01	1·02	1·03
6	1·00	1·00	1·01

In the immediate vicinity of the entrance, Nusselt number behavior should approach the flat plate solution. For n of 1·0, a logarithmic plot of Nu vs. x_0 should show a negative slope of 0·5, whereas 0·46 was actually obtained. The same comparison for other values of n, based on the flat plate solution of Acrivos *et al.* [13] gave similar results. For all values of n, numerical results agree with the flat plate solution within 2 per cent at $x^* = 10^{-4}$. Because of the difference in slopes, agreement is poorer at other values of x^*.

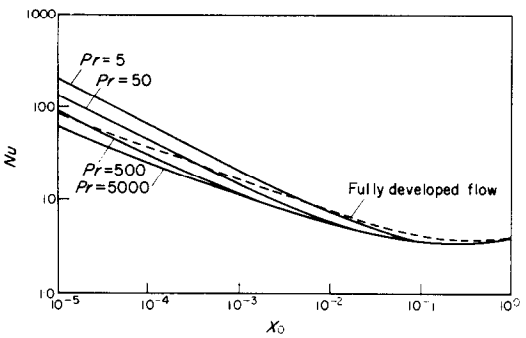

FIG. 3. Variable property Nu for $n = 0{\cdot}7$ and $H = 5{\cdot}0$.

The curves plotted in Fig. 3 for various Pr at $n = 0{\cdot}7$ and $H = 5$ are typical of the results for cooling. The cooling lines all pass below the fully-developed flow line and approach the asymptotic limit from below. This effect is caused by the decreased velocity gradient at the wall that the cooling creates. In heating runs, wall velocity gradients are higher than for constant-property flow, and Nusselt numbers therefore decrease less rapidly toward the limiting fully-developed flow line. Accordingly, all heating curves lie entirely above the fully-developed line. Both cooling and heating lines for all n and Pr approach the asymptotic limit

at x_0 of approximately 1·0. As sufficiently low values of x_0, the lines become straight with slopes essentially equal to those of the constant property lines.

The solution for $n = 1$ was compared with the results of Rosenberg and Hellums [6] for constant property ($Pr = 2$), heating ($Pr = 0{\cdot}2$, $H = 0{\cdot}1$) and cooling ($Pr = 20$, $H = 10$). For the constant property and heating cases, the two solutions agree within 5 per cent over the entire range of x_0. For cooling, the agreement is good at $x_0 > 10^{-3}$, but the line of Rosenberg and Hellums drops much lower at smaller values of x_0 instead of continuing toward the entrance at a constant slope. This behavior corresponds to the results of the present finite difference analysis, and it can be concluded that a much finer grid pattern is necessary if the method is to be reliable in the immediate vicinity of the entrance.

The tabulated results referred to above include coefficients for correlation of the Nusselt number results by equation (10), where $y_p = \ln (Nu/Nu_{min})$ and $z = \ln (1/x_0)$. The correlation is valid over the region $10^{-4} < x_0 < 10^{-1}$). Thus for cooling the correlation applies only up to the point of minimum value. For values of $Nu < 10^{-4}$ these curves can be extrapolated by making them parallel to the constant-property solution whose $Pr = Pr/H$. Results for $n = \frac{1}{3}$ appeared to fall close to those for $n = 0{\cdot}5$. In the absence of more specific information, it is recommended that Nusselt numbers for smaller values of n be obtained from those of $n = 0{\cdot}5$ by applying a factor equal to the ratio of the asymptotic Nusselt numbers.

SUMMARY

The solutions and correlations presented provide a method for calculating entrance-region pressure drops and Nusselt numbers at constant wall temperature for a liquid with a temperature-dependent viscosity. Equation (10) gives the variable-viscosity pressure drop and Nusselt number in terms of the parameters n, Pr and H (the ratio of the wall viscosity to the entering viscosity). The results are valid over the entire entrance region.

ACKNOWLEDGEMENT

This investigation was supported in part by Public Health Service Research Grant No. UI 00270 from the National Center for Urban and Industrial Health.

REFERENCES

1. A. A. McKillop, Heat transfer for laminar flow of non-Newtonian fluids in entrance region of a tube, *Int. J. Heat Mass Transfer* **7**, 853–862 (1964).
2. J. C. Harper and A. F. El Sahrigi, Viscometric behavior of tomato concentrates, *J. Food Sci.* **30**, 470–476 (1965).
3. W. D. Campbell and J. C. Slattery, Flow in the entrance of a tube, *J. Bas. Engng* **85**, 41–46 (1963).
4. D. C. Bogue, Entrance effects and prediction of turbulence in non-Newtonian flow, *Ind. Engng Chem.* **51**, 874–878 (1959).
5. A. H. Shapiro, R. Siegel and S. J. Kline, Friction factor in the laminar entry region of a round tube, Second U.S. Cong. Appl. Mech., ASME, 733–741 (1954).
6. D. E. Rosenberg and J. D. Hellums, Flow development and heat transfer in variable-viscosity fluids, *I/EC Fundamentals* **4**, 417–422 (1965).
7. F. L. Test, Laminar flow heat transfer and fluid flow for liquids with temperature-dependent viscosity, *ASME Paper* 67-WA/HT-8, 1–8 (1967).
8. E. B. Christiansen and S. E. Craig, Jr., Heat transfer to pseudo-plastic fluids in laminar flow, *A.I.Ch.E. Jl* **8**, 154–160 (1962)
9. R. A. Seban, The laminar boundary layer of a liquid with variable viscosity, *Boelter Anniversary Volume*. McGraw-Hill, New York (1964).
10. H. J. Bader, M.S. thesis, University of California, Davis (1964).
11. H. J. Bader, Ph.D. thesis, University of California, Davis (1970).
12. A. Y. Korayem, Ph.D. thesis, University of California, Davis (1965).
13. A. M. Acrivos, J. Shah and E. E. Petersen, *A.I.Ch.E. Jl* **6**, 312–317 (1960).

ECOULEMENT DANS LA RÉGION D'ENTRÉE DE LIQUIDES NON-NEWTONIENS À VISCOSITÉ VARIABLE

Résumé—Une solution numérique a été obtenue pour le problème de l'écoulement d'un fluide non-Newtonien avec une viscosité dépendant de la température dans la région d'entrée d'un tube circulaire. La

solution qui est basée sur une méthode intégrale de calcul de la couche limite dans la région d'entrée immédiate et un schéma de différences finies plus loin en aval, donne les chutes de pression et les nombres de Nusselt en fonction de la distance en aval pour une vitesse d'entrée uniforme et une température constante de la paroi du tube. Un modèle de loi en puissance avec une dépendance de la température du type d'Arrhenius a été employé pour représenter le fluide. Des résultats sont présentés sous la forme de corrélations en fonction des paramètres n, Pr et H (rapport de la viscosité pariétale à la viscosité à l'entrée) à partir desquels des valeurs numériques peuvent être obtenues si l'on connaît les valeurs des constantes de la viscosité de fluide.

ZÄHIGKEITSVERÄNDERLICHE EINLAUFSTRÖMUNG EINER NICHT-NEWTONSCHEN FLÜSSIGKEIT

Zusammenfassung—Für das Problem der Strömung einer nicht-Newtonschen Flüssigkeit mit temperaturabhängiger Zähigkeit im Eintrittsbereich eines runden Rohres wurde eine numerische Lösung gefunden. Die Lösung beruht auf einer integralen Greuzschichtnäherung unmittelbar am Eintritt und auf einem endlichen Differenzenschema in einigem Abstand davon in Strömungsrichtung. Der Druckabfall und die Nusselt-Zahl werden als Funktion des Abstandes in Strömungsrichtung für eine gleichförmige Eintrittsgeschwindigkeit und konstante Rohrwandtemperatur angegeben. Ein Potenzgesetz-Modell mit einer Temperaturabhängigkeit vom Arrhenius-Typ wurde verwendet, um die Flüssigkeit nachzubilden.

Die Ergebnisse werden in Form von Korrelationen in Ausdrücken der Parameter n, Pr und π (Verhältnis der Wand-Viskosität zur Eintritts-Viskosität) angegeben. Numerische Werte können hiervon erhalten werden, wenn die Viskositätskonstanten der Flüssigkeit bekannt sind.

ТЕЧЕНИЕ НЕНЬЮТОНОВСКИХ ЖИДКОСТЕЙ С ПЕРЕМЕННОЙ ВЯЗКОСТЬЮ НА ВХОДНОМ УЧАСТКЕ

Аннотация—Получено численное решение задачи течения неньютоновской жидкости с зависящей от температуры вязкостью на входном участке круглой трубы. Решение, основанное на интегральном методе расчёта пограничного слоя во входной области и конечной разностной схеме вниз по потоку, даёт возможность определить перепады давления и значения критерия Нуссельта как функцию расстояния вниз по потоку для однородной скорости на входе и постоянной температуры стенки трубы. Для описания жидкости использовалась модель степенного закона с температурной зависимостью типа зависимости Аррениуса. Результаты представлены в виде корреляций в параметрах n, Pr и H (отношение вязкости на стенке к вязкости на входе), по которым можно получить численные значения, если известны значения коэффициентов вязкости жидкости.